

# Inelastic X-ray Scattering Studies of the Short-Time Collective Vibrational Motions in Hydrated Lysozyme Powders and Their Possible Relation to Enzymatic Function

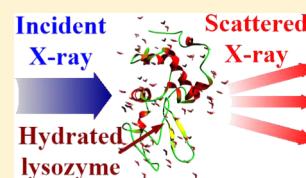
Zhe Wang,<sup>†</sup> Christopher E. Bertrand,<sup>†</sup> Wei-Shan Chiang,<sup>†</sup> Emiliano Fratini,<sup>‡</sup> Piero Baglioni,<sup>‡</sup> Ahmet Alatas,<sup>§</sup> E. Ercan Alp,<sup>§</sup> and Sow-Hsin Chen<sup>\*,†</sup>

<sup>†</sup>Department of Nuclear Science and Engineering, Massachusetts Institute of Technology, Cambridge, Massachusetts 02139, United States

<sup>‡</sup>Department of Chemistry and CSGI, University of Florence, Sesto Fiorentino, Florence, I-50019, Italy

<sup>§</sup>Advanced Photon Source, Argonne National Lab, Argonne, Illinois, 60439, United States

**ABSTRACT:** High-resolution inelastic X-ray scattering was used to investigate the collective vibrational excitations in hydrated lysozyme powders as a function of hydration level and temperature. It is found that the samples with strong enzymatic function are “soft”, in the sense that they exhibit low frequency and large amplitude intraprotein collective vibrational motions on certain length scales. This is not the case for samples with weak or no enzymatic activity. Thus, we identify a possible correlation between the short-time intraprotein collective vibrational motions and the establishment of enzymatic function in hydrated lysozyme powders, and bring new insight to notions of protein “conformational flexibility” and “softness” in terms of these motions.



## INTRODUCTION

After the discovery of the molecular structure of DNA using X-ray diffraction in 1953,<sup>1</sup> the crystallographic structures of many kinds of biological macromolecules, such as DNA and proteins, have been investigated extensively. These studies confirm the crucial role that structure plays in the establishment of the functions of biological macromolecules. Later on, the importance of dynamics in biological activity started to be appreciated.<sup>2</sup> Intuitively, biological macromolecules cannot be totally static, and a “rigid body” cannot have any biological activity. Now it is well accepted that both the structure and dynamics are essential to the enzymatic functions of proteins.<sup>3</sup> Protein dynamics can be considered as any time-dependent change in the protein atomic coordinates. By introducing the concepts of conformational substate and energy landscape, Frauenfelder et al.<sup>4–7</sup> proposed a well-defined picture for the study of protein dynamics. In this framework, the energy landscape describes the potential energy of a protein system as a function of conformational coordinates, i.e., a hyper-surface in the high-dimensional space of the coordinates of all atoms in a protein system.<sup>7</sup> A protein system with a particular energy landscape can assume a very large number of nearly isoenergetic conformational substates. The probabilities of conformational substates and the energy barriers between them are determined by the energy landscape. Due to the complexity of the protein system, the shape of the energy landscape is extremely complicated and can be divided into several tiers. With these ideas, it is natural to divide protein dynamics into two main groups according to the time scale or, equivalently, to the tier of the energy landscape sampled.<sup>8</sup> (1) “Slow” dynamics ( $>1 \mu\text{s}$ ) is characterized by fluctuations between kinetically distinct states that are separated by energy barriers of  $k_B T$  ( $k_B$  is

the Boltzmann constant,  $T$  is temperature), i.e., large-amplitude collective motions. Biological processes like enzyme catalysis and signal transduction occur on this time scale. (2) “Fast” dynamics ( $<1 \mu\text{s}$ , especially on the time scale of  $<1 \text{ ns}$ ) is characterized by fluctuations between conformational substates which are structurally similar and are separated by energy barriers much smaller than  $k_B T$ . Protein motions on this time scale are usually more localized and faster.

Compared with the “slow” functional motions of proteins, the motions corresponding to “fast” dynamics are usually of much smaller amplitude and significantly larger frequency. However, they are somehow connected to the “slow” dynamics that directly correspond to the enzymatic functions of proteins (the so-called “traffic model for conformational space” proposed by Frauenfelder et al.<sup>9</sup> provides some ideas about this connection). In the last few decades, protein dynamics on the “fast” time scale from 1 ps to 1  $\mu\text{s}$  and its relation to biological activities were studied extensively by neutron scattering,<sup>10–16</sup> nuclear magnetic resonance (NMR),<sup>17,18</sup> and Mössbauer spectroscopy.<sup>19,20</sup> The results show a strong correlation (but not sufficient and necessary conditions<sup>16,21,22</sup>) between the biological functions of proteins and atomic self-motion of constituent atoms. Recently, the development of high resolution inelastic X-ray scattering (IXS) techniques has brought a powerful tool for the investigation of the collective motions of condensed matters on very short time scales of  $<1 \text{ ps}$ .<sup>23</sup> Because of the highly coherent signal of the scattered X-ray photons, it is possible by

Received: December 29, 2012

Revised: January 9, 2013

Published: January 9, 2013

using the IXS technique to study the short-time collective vibrational motions of proteins that are difficult to see with neutron scattering. Previously, several papers have been published in this area.<sup>24–27</sup> Liu et al.<sup>24</sup> investigated the temperature dependences of the IXS spectra of lysozyme and bovine serum albumin within the  $Q$  ( $Q$  is the magnitude of the wavevector transfer in scattering experiments) range of about  $20\text{--}30\text{ nm}^{-1}$  by applying the damped harmonic oscillator (DHO) model;<sup>28</sup> Li et al.<sup>25</sup> investigated the temperature dependence of the IXS spectra of casein and  $\alpha$ -chymotrypsinogen within the same  $Q$  range by applying the generalized three effective eigenmode (GTEE) theory;<sup>29</sup> Yoshida et al.<sup>26</sup> studied the sound speed and the damping factor of the hydrated  $\beta$ -lactoglobulin and their dependences on hydration level with the DHO model. In this paper, by applying the GTEE theory, we first present the hydration level dependence of the IXS spectra of hydrated lysozyme samples within both the low  $Q$  range ( $3.5\text{--}13.5\text{ nm}^{-1}$ ) and the high  $Q$  range ( $20\text{--}30\text{ nm}^{-1}$ ). Quite different features are observed in these two different  $Q$  ranges. Second, the temperature dependences of the IXS spectra of hydrated lysozyme samples are examined. Note that here we perform a full analysis in the whole  $Q$  range from 3 to  $30\text{ nm}^{-1}$  with the GTEE theory, which has never been done before. With these results, we find a plausible correlation between the onset of the enzymatic function of lysozyme and the short-time collective vibrational motions. Moreover, we can identify the specific modes that seem to be closely related to the enzymatic function of lysozyme. Also note that we refer “short-time” as the time scale smaller than 1 ps in this study. Furthermore, with the “phonon energy softening” and “phonon population enhancement” observed in the experiment, we may bring new insight to the notions of protein “conformational flexibility” and “softness” in terms of the intraprotein short-time collective vibrational motions.

## EXPERIMENTAL METHODS

The samples studied here are powder samples of lysozyme under different conditions (different hydration levels and temperatures). Lysozyme is an enzyme consisting of 129 amino acid residues which folds into a compact globular structure having an ellipsoidal shape with dimensions  $a \times b \times c = 2.25 \times 1.5 \times 1.5\text{ nm}^3$  and a molecular weight of 14.4 kDa.<sup>30</sup> From a structural point of view, it has five helical regions and five  $\beta$ -sheet regions surrounded by random coils and  $\beta$  turns.<sup>31</sup> The three-dimensional structure of the lysozyme molecule is shown in Figure 1. Lysozyme is part of the human immune system being able to kill gram-positive pathogens by hydrolyzing the peptidoglycans present in their cell walls. Viruses also use this enzyme as an agent to break into host bacterial cells.<sup>32</sup>

Hen egg white lysozyme (L7651), 3 times crystallized, dialyzed, and lyophilized, was purchased from Sigma-Aldrich (Milan). The protein powder was extensively lyophilized to remove any remaining water. The samples were prepared by isopiastically exposing the dry powder to water vapor in a closed chamber for different times to achieve four different hydration levels,  $h = 0.06, 0.16, 0.33$ , and  $0.43$ . The temperature was maintained at  $5\text{ }^\circ\text{C}$  during the hydrating procedure. The level of hydration was controlled by varying the exposure time.

The high-resolution inelastic X-ray scattering (IXS) experiment was performed at the 3-ID-XSD beamline at the Advanced Photon Source (APS), Argonne National Laboratory, where the selected incident monochromatic X-ray beam has an energy of 21.657 keV. The X-ray scattering spectra were



**Figure 1.** Three-dimensional structure of lysozyme.  $\alpha$ -Helices are denoted by red coils,  $\beta$ -sheets are denoted by yellow sheets, and turns are shown in green color.

simultaneously collected by four spherically shaped diced-silicon crystal analyzers.<sup>33–35</sup> The energy resolution of the spectrometer is roughly 2.0 meV for three of the four analyzers, and about 3.2 meV for the other analyzer. IXS is a powerful tool for investigating the collective vibrational motions of atoms. In this experiment, the measured magnitude of the wavevector transfer  $Q$  was in the range  $2.8\text{--}32\text{ nm}^{-1}$  and the energy transfer,  $E$ , covers a window from  $-25$  to  $25\text{ meV}$ . In general, a measured IXS spectrum  $I_m(Q, E)$  can be expressed as the convolution  $I_m(Q, E) = S_m(Q, E) \otimes R(E)$ , where  $S_m(Q, E)$  is the dynamic structure factor of the protein sample and  $R(E)$  the energy resolution function of the IXS spectrometer. This energy resolution function is well modeled by a pseudo-Voigt function:<sup>33</sup>

$$R(E) = I_0 \left[ \frac{2\eta}{\pi\Gamma} \frac{1}{1 + 4\left(\frac{E}{\Gamma}\right)^2} + (1 - \eta) \frac{2}{\Gamma} \left( \frac{\ln 2}{\pi} \right)^{1/2} e^{-4\ln 2(E/\Gamma)^2} \right] + c_{bg} \quad (1)$$

One can find that  $R(E)$  is composed of a Gaussian peak and a Lorentzian peak.  $\eta$  is the mixing ratio of the Lorentzian peak and the Gaussian peak,  $\Gamma$  is the fwhm for both peaks, and  $c_{bg}$  is the background.

The IXS spectra can be analyzed adopting the generalized three effective eigenmode (GTEE) theory.<sup>29</sup> GTEE is a generalization of the three effective eigenmode theory,<sup>36</sup> which is applicable to simple liquids, to multicomponent systems like proteins. Previous studies have successfully applied this theory to investigate different biomaterials such as hydrated lipid bilayers,<sup>37,38</sup> liquid crystalline DNA,<sup>39–41</sup> and other globular proteins.<sup>25</sup> Within the GTEE framework, the normalized dynamic structure factor (NDSF) can be written as

$$\begin{aligned} \frac{S_{\text{GTEE}}(Q, E)}{S(Q)} &= \text{Re} \left[ \frac{S_{\text{GTEE}}(Q, z)}{S(Q)} \right]_{z=iE} \\ &= \frac{1}{S(Q)} \text{Re} \left[ z + \frac{f_{un}^2(Q)}{z + z_u(Q) + \frac{f_{un}^2(Q)}{z + z_r(Q)}} \right]_{z=iE}^{-1} \end{aligned} \quad (2)$$

where  $f_{un}(Q) = Qv_0(Q)/S(Q)^{1/2}$ ,  $v_0(Q)$  is the generalized thermal velocity, and  $S(Q)$  is the static structure factor, which can be experimentally measured. The subscripts  $u$ ,  $n$ , and  $T$

denote the momentum, number density, and temperature modes, respectively. The parameters  $f_{un}$  and  $f_{uT}$  are coupling constants between the  $u$  and  $n$  modes and the  $u$  and  $T$  modes, while  $z_u$  and  $z_T$  are the decay rates of the  $u$  and  $T$  modes.

The continued fraction form of the NDSF from the GTEE theory, eq 2, can be transformed into an expression that exhibits three generalized hydrodynamic modes:

$$\frac{S_{\text{GTEE}}(Q, E)}{S(Q)} = \frac{1}{\pi} \left[ A_h \frac{\Gamma_h}{\Gamma_h^2 + E^2} + A_s \frac{\Gamma_s + b(E + \Omega_s)}{\Gamma_s^2 + (E + \Omega_s)^2} + A_s \frac{\Gamma_s - b(E - \Omega_s)}{\Gamma_s^2 + (E - \Omega_s)^2} \right] \quad (3)$$

In eq 3, the first term represents quasi-elastic scattering (Rayleigh peak) and the last two terms represent inelastic scattering (Brillouin peaks). The fractional area of the Rayleigh peak is  $A_h = 1 - 2A_s$ , where  $A_s$  is the fractional area of the Brillouin peak. The widths of the Rayleigh peak and the Brillouin peaks are given by  $\Gamma_h$  and  $\Gamma_s$ , respectively, while  $\pm\Omega_s$  are the positions of Brillouin peaks, i.e., the energy of the phonon-like excitation (or equivalently the vibrational frequency). Notice that we use the quantum-mechanical term “phonon-like excitation” to represent the short-time collective vibrational motion mode in protein in this study. In the following parts, we will use “phonon” instead of “phonon-like excitation” for short. The six parameters in eq 3 are functions of the four  $Q$ -dependent parameters:  $f_{un}(Q)$ ,  $z_u(Q)$ ,  $z_T(Q)$ , and  $f_{uT}(Q)$ , found in eq 2.<sup>29</sup>

In contrast to  $S_{\text{GTEE}}(Q, E)$ , which comes from a classical theory, the measured spectrum  $S_m(Q, E)$  is not symmetric with respect to energy gain ( $-E$ ) and energy loss ( $+E$ ) due to quantum effects. Consequently, it is necessary to multiply the theoretical  $S_{\text{GTEE}}(Q, E)$  by the detailed balance factor  $R_d(E) = \exp(E/2k_B T)$ <sup>42</sup> before comparing the theoretical results with the experimentally measured spectra.

In the following section, we will show the analysis of the IXS spectra of different lysozyme samples extracted by applying the GTEE theory, and discuss their possible relation to the enzymatic activity of lysozyme.

## RESULTS AND DISCUSSION

**General Features.** Measured IXS spectra for the protein sample at  $T = 300$  K and  $h = 0.33$  are shown in Figure 2 along with theoretical NDSFs calculated from fits of the GTEE model. We use the logarithmic scale here to emphasize the side-peaks which are closely related to the collective excitation features. The overall agreement between the measured and calculated NDSFs is satisfactory. Notice that, for the case of  $Q = 16.5 \text{ nm}^{-1}$ , which is shown in Figure 2b, the extracted  $\Omega_s$  is equal to 0, which means the phonons are overdamped in this case. Figure 3 shows the calculated NDSFs at different  $Q$  values. In the case of  $Q = 16.5 \text{ nm}^{-1}$ , the  $Q$  value is close to the diffraction peak of the structure factor  $S(Q)$  (shown in Figure 4d) and the effect of de Gennes narrowing<sup>43,44</sup> of the Rayleigh peak can be seen in Figure 3 clearly. Notice that the extracted width of the Rayleigh peak  $\Gamma_h$  (of the order of 0.1 meV) is much smaller than the instrumental energy resolution of 2 meV (as shown in Figure 2). In the GTEE theory, the Rayleigh peak and two Brillouin peaks are coupled, so that we can extract some information about the Rayleigh peak.

Figure 4a shows the dispersion relation of the phonon-like excitations for the sample at  $T = 300$  K and  $h = 0.33$ . The high-

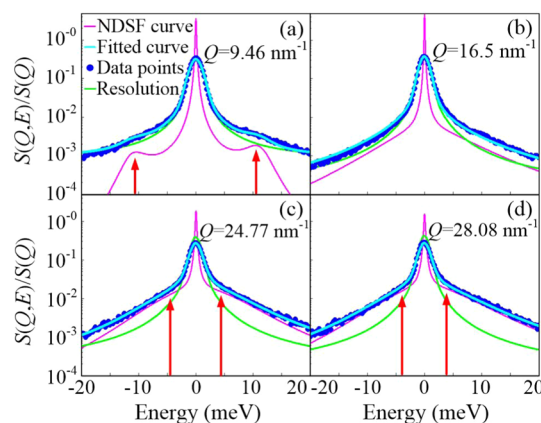


**Figure 2.** IXS spectra for the sample at  $T = 300$  K and  $h = 0.33$  in logarithmic scale for different  $Q$  values ( $Q = 9.46, 16.5, 24.77$ , and  $28.08 \text{ nm}^{-1}$  correspond to parts a, b, c, and d, respectively). The blue points are the measured spectral data points. The pink line is the extracted NDSF (multiplied by the detailed balance factor), as given by  $S_{\text{GTEE}}(Q, E) \cdot R_d(E)/S(Q)$ . The green line shows the energy resolution function of the spectrometer. The cyan line is the fitted spectral intensity,  $I_{\text{GTEE}}(Q, E) = [S_{\text{GTEE}}(Q, E) \cdot R_d(E)/S(Q)] \otimes R(E)$ . The red arrows indicate the positions of the Brillouin peaks.

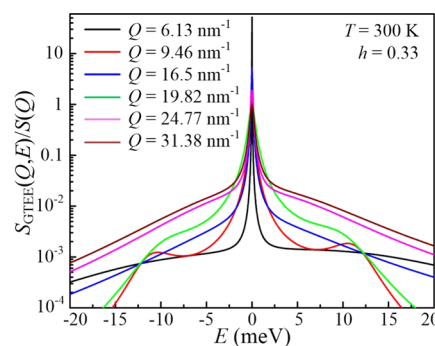


**Figure 3.** The extracted NDSFs for the sample at  $T = 300$  K and  $h = 0.33$  in logarithmic scale at different  $Q$  values. The black line, red line, blue line, green line, magenta line, and brown line correspond to  $Q$  values of 6.13, 9.46, 16.5, 19.82, 24.77, and 31.38  $\text{nm}^{-1}$ , respectively. In the case of  $Q = 16.5 \text{ nm}^{-1}$  (indicated by the blue line), the  $Q$  value is close to the diffraction peak of the structure factor  $S(Q)$  and the de Gennes narrowing can be seen clearly.

frequency longitudinal sound speed  $v_L$  of the hydrated protein sample can be estimated with the data points within the  $Q$  range below  $6.5 \text{ nm}^{-1}$ .<sup>26,27</sup> For this sample, the resulting  $v_L$  is approximately 2978 m/s. Comparing this with other IXS measurements on different hydrated proteins, this value is close to that of  $\beta$ -lactoglobulin at  $h = 0.5$  (2895 m/s),<sup>26</sup> and is less than that of cytochrome  $c$  at  $h = 0.2$  (3458 m/s).<sup>27</sup> A more accurate  $v_L$  value could be calculated only by measuring the region below  $Q = 6.5 \text{ nm}^{-1}$  in more detail (i.e., a greater number of experimental points). For the dispersion relation in larger  $Q$  range, one can find there is a valley around  $Q = 15 \text{ nm}^{-1}$  that is close to the diffraction peak of the structure factor. Similar features were also observed in many other kinds of biomaterials like hydrated lipid bilayer<sup>37</sup> and liquid crystalline DNA.<sup>39</sup> For the  $Q$  range larger than  $20 \text{ nm}^{-1}$ , there are no obvious features observed, and it seems that the value of  $\Omega_s$  fluctuates in a small range with the increase of  $Q$ . However, both this study and a previous study on two different kinds of hydrated globular proteins (casein and  $\alpha$ -chymotrypsinogen)<sup>25</sup>



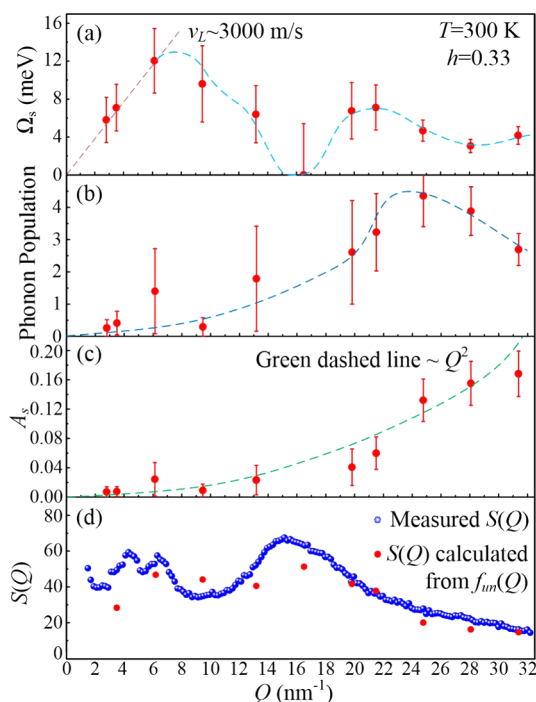


**Figure 4.** For the sample at  $T = 300$  K and  $h = 0.33$ : (a) measured dispersion relation of phonon-like excitations, (b) phonon population, (c) fractional area of the Brillouin peaks  $A_s$ , and (d) the structure factor  $S(Q)$ . The dashed lines are drawn to guide the eyes. In panel d, the measured  $S(Q)$  data are indicated by blue circles, and the calculated  $S(Q)$  values are indicated by red circles.

show a small valley around  $Q = 28 \text{ nm}^{-1}$ . For these three globular proteins studied, they have very different tertiary structures but similar secondary structures. Furthermore, the  $Q$

values between 20 and  $30 \text{ nm}^{-1}$  correspond to the length scale range of about  $2\text{--}3 \text{ \AA}$ , which is comparable to the typical length scale of the spatial order of protein secondary structures ( $4\text{--}5 \text{ \AA}$ ). Thus, we conjecture that this small valley may be related to the structure and dynamics of the protein secondary structure.

From Figure 4c, one can find the fractional area of the Brillouin peak  $A_s$  increases nonmonotonically over the experimental  $Q$  range. This makes a major contribution to the similar increase in phonon population  $n_p$ , which can be related to  $A_s$  by  $n_p(Q) \propto A_s(Q) \cdot S(Q)$ , over the similar  $Q$  range (as shown in Figure 4b). This increase of  $A_s$  may be explained partially as follows: for a system constituted by harmonic oscillators, the relative intensity of the quasi-elastic scattering peak  $A_h$  can be taken as approximately proportional to the Debye–Waller factor  $\exp(-Q^2\langle x^2 \rangle)$ .<sup>45</sup> Since  $A_h + 2A_s = 1$ , one finds that  $A_s = [1 - \exp(-Q^2\langle x^2 \rangle)]/2$ , and thus,  $A_s$  increases with increasing  $Q$ . If we expand the Debye–Waller factor for small  $Q^2$ , we find that  $A_s$  is proportional to  $Q^2$ . However, Figure 4c does not show a strict  $Q^2$  dependence. The reason probably resides in (1) the anharmonic components in the molecular motions, (2) the nonperiodic structure of the protein–water system, and (3) higher order terms in the expansion of  $A_s$ , which cannot be ignored as  $Q$  becomes larger.

Figure 4d shows the measured structure factor  $S(Q)$  of the sample. The diffraction peak at around  $Q = 15 \text{ nm}^{-1}$  arises from the spatial order of the secondary structure ( $\beta$ -sheet average distance and  $\alpha$ -helix repeat and width).<sup>46</sup> And it is around here the “valley” in dispersion relation and de Gennes narrowing happen. In addition, one can calculate the structure factor  $S(Q)$  in an absolute scale using the relation  $S(Q) = Q^2 v_0^2(Q) / f_{un}^2(Q)$ ,<sup>29</sup> provided that  $v_0(Q)$  is calculated with the GTEE multiatom model using known atomic form factors and the atomic composition of lysozyme. The calculated  $S(Q)$  values are indicated by red circles in Figure 4d.

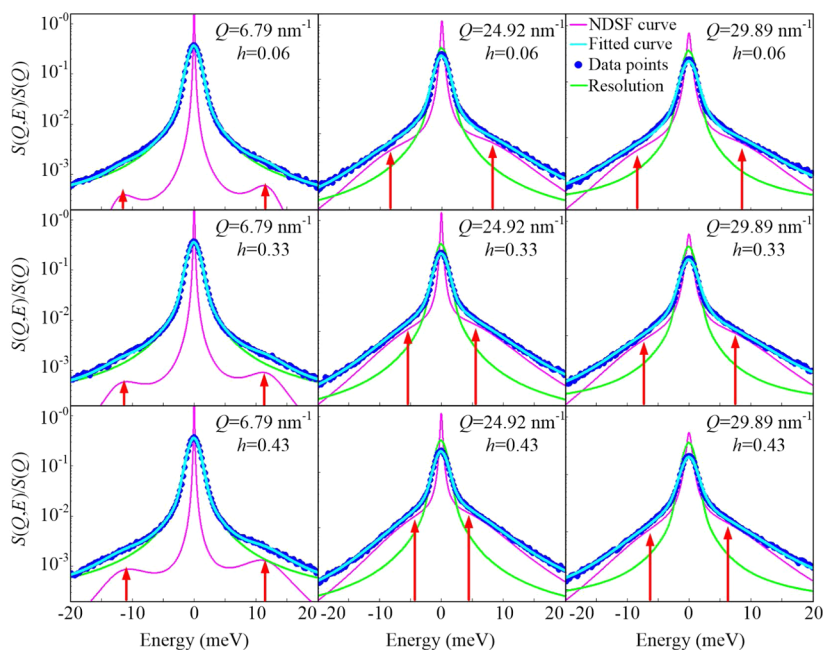


**Figure 5.** IXS spectra in logarithmic scale at three different  $Q$  values ( $Q = 6.79, 24.92$ , and  $29.89 \text{ nm}^{-1}$  from left to right) and at the three hydration levels ( $h = 0.06, 0.33$  and  $0.43$ , from top to bottom). The blue points are the measured spectral data points. The pink line is the extracted NDSF (multiplied by the detailed balance factor), as given by  $S_{\text{GTEE}}(Q, E) \cdot R_d(E) / S(Q)$ . The green line shows the energy resolution function of the spectrometer. The cyan line is the fitted spectral intensity,  $I_{\text{GTEE}}(Q, E) = [S_{\text{GTEE}}(Q, E) \cdot R_d(E) / S(Q)] \otimes R(E)$ . The red arrows indicate the positions of the Brillouin peaks.

The sample studied in this section is in its native state and has special meaning for this study. This study involves many times IXS experiments, and for each experiment, the native lysozyme samples at  $T = 300$  K and  $h = 0.33$  were measured as a “reference sample”. The average values of  $\Omega_s$  and  $A_s$  for different experiments are consistent, and the relative differences are smaller than 10%.

**Hydration Level Dependence.** Hydration water plays a crucial role in protein thermodynamics and dynamics.<sup>47,48</sup> At its physiological temperature, the globular protein lysozyme only functions as an enzyme when its hydration level is higher than the threshold value of  $h = 0.2$ – $0.25$  (g of  $H_2O$ /1 g of dry lysozyme).<sup>47</sup> The hydrogen-bonding sites on the surface of the protein are completely saturated with water at this hydration level. Above this level, water begins to cover the nonpolar regions of the surface as well. Moreover, neither hydration nor dehydration significantly alter the protein’s conformation, which is traditionally considered to be one of the most important factors for determining the biological function of proteins.<sup>48</sup> These results suggest that the hydration level is an ideal “control parameter” for switching on and off the enzymatic function of lysozyme without significantly altering its conformation. Therefore, by changing the hydration level, we can study the relationship between the dynamics of the protein and its enzymatic function. In previous papers, the short-time collective dynamics of different proteins were studied at different hydration levels.<sup>26,27,49,50</sup> However, the relationship between the short-time intraprotein collective motions, the hydration level, and the onset of the enzymatic function were not clearly elucidated. In this section, we present inelastic X-ray scattering results for lysozyme at four different hydration levels,  $h = 0.06, 0.16, 0.33$ , and  $0.43$ , in order to clarify the above-mentioned relationship. We stress that  $h = 0.06$  and  $0.16$ , the two lower hydration levels studied, are well below the threshold of enzymatic activity for lysozyme, while the other two selected hydrations are well above it.

Typical measured IXS spectra as well as the theoretical spectra calculated by applying the GTEE theory for samples with different hydration levels are shown in Figure 5. It can be found that the agreement between the measured spectra and the calculated spectra is good. Figure 6 shows the change of the

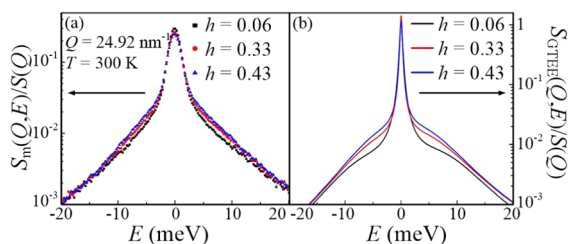


**Figure 6.** (a) Measured spectra and (b) theoretical spectra calculated by the GTEE theory for three samples with different hydration levels  $h = 0.06, 0.33$ , and  $0.43$  at  $Q = 24.92 \text{ nm}^{-1}$ . The hydration levels of  $0.06, 0.33$ , and  $0.43$  are indicated by black color, red color, and blue color, respectively.

spectrum induced by changing hydration level at  $Q = 24.92 \text{ nm}^{-1}$  and  $T = 300$  K. Figure 6a shows the measured spectra  $S_m(Q, E)/S(Q)$  for different hydration levels  $h = 0.06, 0.33$ , and  $0.43$ . Notice that  $S_m(Q, E)/S(Q)$  is equal to the convolution of the energy resolution function of the instrument and the theoretically calculated spectrum  $S_{\text{GTEE}}(Q, E)/S(Q)$ , which is

shown in Figure 6b. From Figure 6a, one can find that the change of spectrum induced by changing  $h$ , especially the change in Brillouin peaks, although very small, can be seen under logarithmic scale. And from Figure 6, it can be found that the theoretical spectrum obtained by applying the GTEE theory correctly reflects such small change in the measured spectrum.

Figure 7 shows the dispersion relations of the phonon-like excitations (a), the phonon population (b), and the fractional

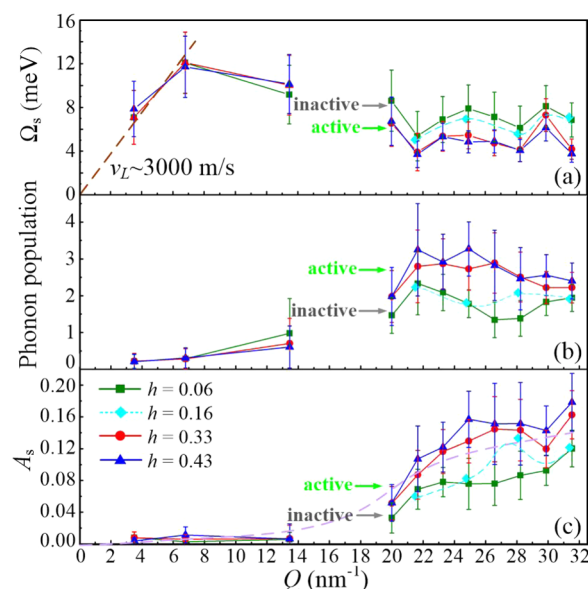


**Figure 7.** (a) Measured dispersion relations of phonon-like excitations, (b) phonon population, and (c) fractional area of the Brillouin peaks  $A_s$  at the four measured hydration levels. Green squares, cyan rhombuses, red circles, and blue triangles indicate  $h = 0.06, 0.16, 0.33$ , and  $0.43$ , respectively. Within the  $Q$  range of  $20$ – $31 \text{ nm}^{-1}$ , the phonon energies are softened significantly and the phonon population is enhanced when crossing the minimum hydration level ( $h = 0.2$ – $0.25$ ) required for the enzymatic function of lysozyme. However, within the  $Q$  range of  $3.5$ – $13.5 \text{ nm}^{-1}$ , such phenomena were not observed. The dashed lines are drawn to guide the eyes. Notice that we only measured one set of  $Q$  values (four  $Q$  values) for the sample of  $h = 0.16$  due to the limited beamtime. In order to make the figure clearer, we did not add an error bar for this hydration level case.

area of the Brillouin peaks  $A_s$  (c) at the four measured hydration levels. Within the  $Q$  range of  $20$ – $31 \text{ nm}^{-1}$ , the phonons exhibit a substantial softening ( $\sim 2 \text{ meV}$ ) for the higher hydration levels ( $h = 0.33$  and  $0.43$ ), as seen from Figure 7a. Additionally, the phonon population and the fractional area of the Brillouin peaks  $A_s$  are significantly enhanced at these hydration levels, as shown in Figure 7b and c. It is also notable that the phonon energies show little change when the hydration level is increased from  $h = 0.33$  to  $h = 0.43$ , whereas the phonon population increases slightly between these hydration levels. In contrast, in the  $Q$  range of  $3.5$ – $13.5 \text{ nm}^{-1}$ , a softening of the phonon energy and an enhancement of the phonon population are not observed, as seen from Figure 7.

The above arguments suggest that the collective vibrational motions within the  $Q$  range from  $20$  to  $31 \text{ nm}^{-1}$  may be closely related to the onset of lysozyme’s enzymatic function, since lysozyme is enzymatically inactive for  $h = 0.06$  and  $0.16$  and enzymatically active for  $h = 0.33$  and  $0.43$ . We can use the concept of “conformational flexibility” to characterize the qualitative effects of these changes in phonon energies and

populations. Lower phonon energies and an enhancement in the phonon population correspond to greater conformational flexibility, because less energy is required to excite collective motion and a greater phonon population is indicative of larger amplitude vibrations. Thus, lysozyme may only function as an enzyme when it is “soft”. The small enhancement in the phonon population observed between  $h = 0.33$  and  $0.43$  may be related to the fact that the enzymatic activity of lysozyme continues to increase with increasing hydration for  $h > 0.2$ .<sup>47</sup> In contrast, due to the hydration level independence of phonon energies and the phonon population in the lower  $Q$  range below  $13 \text{ nm}^{-1}$ , one may conjecture that the collective vibrational motions on length scales larger than  $5 \text{ \AA}$  are not so closely related to the enzymatic function of lysozyme.

The reason why such phonon energy softening and population enhancement happen may be explained as follows. According to Wang et al.<sup>51</sup> (see also Doster et al.<sup>52</sup>), protein–water interaction can be sketched by Figure 8: Without water

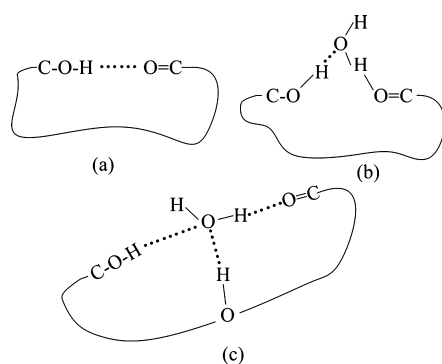


**Figure 8.** Protein–water interaction: (a) without water, hydrophilic interactions are saturated internally; (b) two functional groups bridged by a single water molecule; (c) three functional groups bridged by a single water molecule.<sup>51,52</sup> The hydrogen bonds are denoted by dotted lines.

(Figure 8a), hydrophilic interactions have to be saturated internally. If water molecules exist, water allows the structure to expand. The optimal hydrogen bond configurations for the coupling of two and three functional sites are shown in Figure 8b and c, respectively. One can find that, with protein–water interaction, the accessible protein conformational space for collective motions increases, while the total bond energy per unit volume decreases, since the free volume for motions increases and the hydrogen bond, which increases in number, is weaker than a typical covalent bond. These two mechanisms may cause the increase of the amplitude of the collective motion and the moderation of the collective vibration frequency, i.e., the phonon population enhancement and phonon energy softening. When the hydration level is larger than  $0.25$ , the polar sites on the protein surface are saturated completely with water molecules. Thus, in this case, the above two mechanisms are also “saturated”. This may be the reason why there is no significant change in phonon energy and population when changing hydration level from  $0.33$  to  $0.43$ .

Figure 9 shows the widths of the Brillouin peaks  $\Gamma_s$  as a function of  $Q$ . The width  $\Gamma_s$  does not change with the hydration level in this experiment. This indicates that the value of  $\Gamma_s$  is not very sensitive to the biological function of the protein. The extracted width of the Rayleigh peak  $\Gamma_h$  does not show any  $h$  dependence either. The collective motions of the hydrated

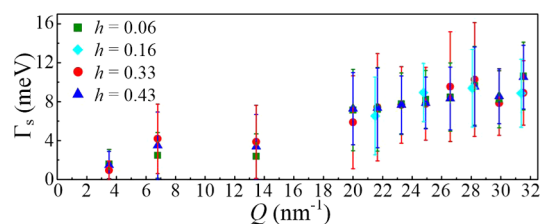


**Figure 9.** Phonon damping constant  $\Gamma_s$  at the four measured hydration levels. The symbols correspond to the same hydration levels as in Figure 7. Notice that  $\Gamma_s$  appears to be insensitive to the hydration level, and thus may be unrelated to the biological function of the protein.

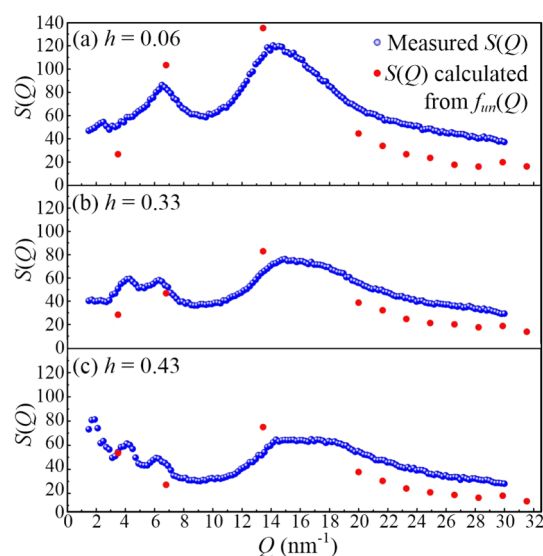
proteins are damped. In the GTEE model, this damping is captured by the parameters  $\Gamma_s$  and  $\Gamma_h$ , which, in the time domain, are the damping constants of the phonon mode and heat mode. One can identify a two-step relaxation in the protein dynamics, since  $\Gamma_s$  is typically much larger than  $\Gamma_h$ . In GTEE theory, both of the two relaxation processes are exponential. However, there are indications that the actual long-time decays of the protein dynamics may be logarithmic and beyond the energy resolution of the IXS spectrometer used in this study.<sup>53</sup> Even so, the GTEE model constitutes a good approximation considering the IXS energy resolution.

In the limit  $Q \rightarrow 0$ , the intensity of X-ray scattering from a single atom is proportional to  $Z^2$ , where  $Z$  is the atomic number. Consequently, a non-negligible fraction of the measured scattering is due to oxygen atoms in the hydration water. Recently, the collective motions of the protein hydration water were studied both by molecular simulation<sup>54</sup> and Brillouin neutron scattering.<sup>49</sup> The hydration levels studied in this paper are  $h = 0.06, 0.16, 0.33$ , and  $0.43$ , which are smaller than or close to the hydration level required to create monolayer coverage of the protein molecule ( $h \sim 0.4$ ), and are much smaller than the hydration levels studied in the above-mentioned studies where  $h = 0.5, 0.68$ , and  $1$ . Thus, in the current study, water molecules cannot form a well-defined second shell around the protein molecule and cannot form a three-dimensional water–water hydrogen-bond network. In addition, within the short time scale probed by IXS, which is typically several hundred femtoseconds, the hydration water molecules are bound to the protein surface and vibrate. Therefore, taking into account the phonon energy and population associated with short time dynamics of protein, the contribution from the hydration water does not need to be considered separately, in the lowest order of approximation.

As mentioned previously, one can calculate the static structure factor in an absolute scale using the relation  $S(Q) = Q^2 v_0^2(Q) / f_{un}^2(Q)$ ,<sup>29</sup> provided that  $v_0(Q)$  is calculated with the GTEE multiatom model using known atomic form factors and the atomic composition of lysozyme. Figure 10 shows the calculated and measured  $S(Q)$  in the relevant  $Q$  range, which are in good agreement.

**Temperature Dependence.** A large number of studies show that the hydrated proteins undergo a dynamic transition at the transition temperature  $T_D$ .  $T_D$  varies from  $200$  to  $240 \text{ K}$  for different kinds of proteins and different hydration levels.<sup>10–13,55</sup> Below  $T_D$ , protein is solid-like and behaves harmonically, while, above  $T_D$ , protein exhibits anharmonic motions with larger mean square displacement. Experiments show that protein is functional at the temperatures above  $T_D$  and its biological activity increases with the increase of

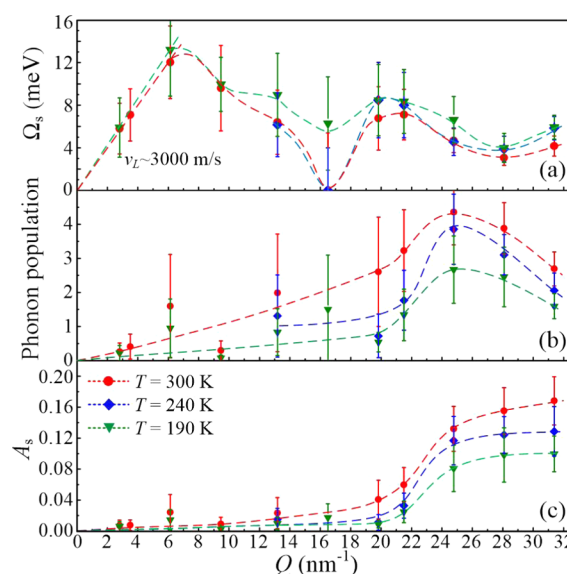




**Figure 10.** Comparisons between the theoretically calculated structure factor (red circles) and the measured structure factor (blue circles) at the three measured hydration levels ( $h = 0.06, 0.33$ , and  $0.43$  from top to bottom).

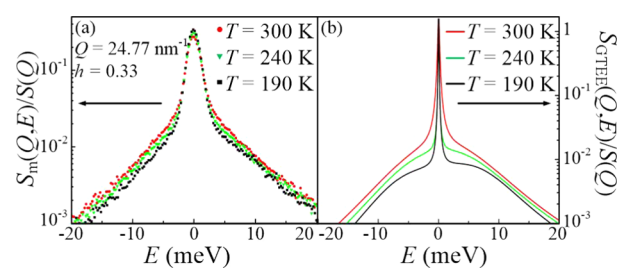
temperature in a certain range, while, for temperatures below  $T_D$ , the biological functions of protein nearly disappear.<sup>56</sup> Therefore, by investigating the temperature dependence of the IXS spectrum of protein, one can study the relationship between the dynamics of protein and its enzymatic function. In a previous study,<sup>24</sup> the temperature dependence of the IXS spectrum of lysozyme was investigated with the damped harmonic oscillator (DHO) model<sup>28</sup> within the  $Q$  range  $19\text{--}32\text{ nm}^{-1}$  and the phonon energy softening was observed when crossing  $T_D$  from below (the temperatures studied are 180, 220, and 250 K in that paper). In this section, we present inelastic X-ray scattering experimental results for lysozyme with  $h = 0.33$  at three different temperatures,  $T = 190$  (below  $T_D$ ), 240, and 300 K (above  $T_D$ ), by applying the GTEE theory, for the following reasons: (1) The DHO model is an approximation of the GTEE model that neglects quasielastic scattering processes and corresponds to the limit in which  $f_{uT}$  tends to zero. Thus, in the DHO model, a phenomenological  $\delta$ -function is assumed to represent the central peak (i.e., the Rayleigh peak) of the IXS spectrum. However, in our experience, for  $Q$  larger than  $20\text{ nm}^{-1}$ , the difference between the width of the measured Rayleigh peak (the convolution of the theoretically calculated Rayleigh peak and the energy resolution function) and the width of the energy resolution function cannot be ignored, so the  $\delta$ -function assumption is no longer very satisfied in this case. In contrast, the GTEE theory does not need to assume such a  $\delta$ -function, and thus is expected to be able to give a better fitting. (2) By analyzing all the data in a consistent way, we can compare the phonon energies and population of the hydration level dependence case and temperature dependence case directly, which is important for obtaining quantitative conclusions. (3) In the above-mentioned reference<sup>24</sup> by Liu et al., the dispersion relations within the  $Q$  range  $3\text{--}9\text{ nm}^{-1}$  were also measured. However, the result shows a flat relation which seems unphysical; this may be due to a very small “spurious peak” in the energy resolution function around 10 meV. In this study, we fix this problem and more accurate dispersion relations in the full  $Q$  range from  $2.8$  to  $31\text{ nm}^{-1}$  are extracted.

Figure 11 shows the dispersion relations of the phonon-like excitations (a), the phonon population (b), and the fractional



**Figure 11.** (a) Measured dispersion relations of phonon-like excitations, (b) phonon population, and (c) fractional area of the Brillouin peaks  $A_s$  at the three temperatures. Red circles, blue rhombuses, and green triangles indicate  $T = 300, 240$ , and  $190\text{ K}$ , respectively. When crossing the dynamical transition temperature  $T_D$  from below, the phonon energies are softened within the  $Q$  range of about  $13.5\text{--}31\text{ nm}^{-1}$ , and the phonon population is enhanced in the whole measured  $Q$  range. The dashed lines are drawn to guide the eyes. We did not measure the data within the  $Q$  range below  $10\text{ nm}^{-1}$  for the sample at  $T = 240\text{ K}$  due to the limited beamtime.

area of the Brillouin peaks  $A_s$  (c) at the three measured temperatures. Figure 12 shows the change of the IXS spectrum



**Figure 12.** (a) Measured spectra and (b) theoretical spectra calculated by the GTEE theory for the lysozyme sample with  $h = 0.33$  at three different temperatures  $T = 300, 240$ , and  $190\text{ K}$  at  $Q = 24.77\text{ nm}^{-1}$ . The temperatures of 300, 240, and 190 K are indicated by red color, green color, and black color, respectively.

induced by changing temperature for the sample with  $h = 0.33$  and at  $Q = 24.77\text{ nm}^{-1}$ . From Figure 11, one can find, when increasing the temperature from 190 to 300 K, the phonon energy softening happens within the  $Q$  range of about  $13.5\text{--}31\text{ nm}^{-1}$ , and the phonon population enhancement happens in all the measured  $Q$  values. Compared with the previous study by Liu et al.,<sup>24</sup> within the  $Q$  range of about  $20\text{--}30\text{ nm}^{-1}$ , the softening observed here from the  $T = 190\text{ K}$  case to the  $T = 300\text{ K}$  case is even weaker than that presented in ref 24 from the  $T = 180\text{ K}$  case to the  $T = 250\text{ K}$  case. This “weaker” softening is similar to the situation observed in another study<sup>25</sup>

on two different proteins by applying the GTEE theory. This difference may be due to the different models used by these researchers. In addition, it is notable that in the  $Q$  range 20–31  $\text{nm}^{-1}$  the softening from the 190 K case to the 300 K case is weaker than that in changing hydration level from 0.06 to 0.33 (see Figure 7). This may be because in this case the number of hydrogen bonds does not change when changing the temperature; thus, the average bond energy per unit volume does not change as strong as that in changing hydration level from 0.06 to 0.33. On the other hand, the enhancements of phonon population and the value of  $A_s$  are significant and clear. This may be because at higher temperature it is easier to excite modes; thus, one can observe a larger phonon population. In fact, it was shown in a previous study that both low temperature and dehydration leads to glassy state.<sup>52</sup> Notice that, in the  $Q$  range above 20  $\text{nm}^{-1}$ , the coherent dynamic structure factors of protein at temperatures lower than  $T_D$  and protein with hydration levels less than 0.2 exhibit similar features (for example, from Figures 6 and 12, one can find the similarity of the NDSFs of sample at  $T = 190$  K and sample at  $h = 0.06$  at  $Q$  around 24  $\text{nm}^{-1}$ ); this suggests that the intraprotein collective motions of these two cases are similar to some extent.

One may argue that the motions corresponding to the relatively large  $Q$  values (for example,  $Q > 14 \text{ nm}^{-1}$ ) are localized motions rather than collective motions, for the reasons that there is no strong correlation between phonon energy and wavenumber in this  $Q$  range (this is usually a feature of localized motions<sup>57</sup>), and in short-time domain and large  $Q$  region, localized motions, such as methyl rotation, become important. In fact, X-ray scattering is highly coherent and mainly detects the motions of heavy atoms in the sample; therefore, the scattered spectrum is dominated by the collective motions of the sample if they exist, and the individual motions, especially the fast motions of hydrogen atoms, are hardly seen. In addition, for the case in this study, the portion of the dispersion relation in the high  $Q$  range ( $Q > 14 \text{ nm}^{-1}$ ) seems to be an extension of the acoustic branch (as shown in Figure 4a), in which the longitudinal modes are in some sense propagating modes. From this section, we identify the  $Q$  range of 13.5–31  $\text{nm}^{-1}$  within which significant phonon energy softening and population enhancement happen simultaneously. This  $Q$  range corresponds to wavelengths in the range 2.1–4.5 Å, which are comparable to the typical length scales of the spatial order of the protein secondary structures (for example, the distance of the  $\beta$ -sheet is about 4 Å, and the width and repeat of the  $\alpha$ -helix is about 5 Å<sup>58</sup>). Therefore, we conjecture that the phonon-like excitations in this range mainly reflect the intraprotein motions, especially the motions associated with the secondary structure of the protein. Notice that the collective motions in this  $Q$  range involve only a few amino acid residues which include dozens of atoms. This “intra-secondary-structure collective motion” is a more localized motion compared to some other short-time collective motions studied previously, such as the hinge motion in lysozyme<sup>59</sup> and the short-time structural collective motions in cytochrome *c*.<sup>60</sup> For the case of hydration level dependence, the dispersion relations within  $Q = 13.5$ –20  $\text{nm}^{-1}$  were not measured. However, from Figure 7, one can find it is quite possible that  $Q = 20 \text{ nm}^{-1}$  is not the lower end point of the phonon softening and population enhancement. Thus, these two phenomena are expected to extend into the  $Q$  region between 13.5 and 20  $\text{nm}^{-1}$ . Therefore, basically the above statement also holds for the case of hydration level dependence.

It is noticeable that the phonon softening and population enhancement become inconspicuous or even disappear when  $Q$  is smaller than 13.5  $\text{nm}^{-1}$  for both the hydration level case and the temperature case. In this  $Q$  range, the wavelength of the collective motion,  $\lambda = 2\pi/Q$ , exceeds the length scale of the spatial order of the protein secondary structures. And it is comparable to the length scale of the protein molecule when  $Q \sim 5 \text{ nm}^{-1}$ . Consequently, we can conjecture that, when  $Q$  is sufficiently small, the relative intensities of the intersecondary-structure phonons and the interprotein phonons will be dominant, while the relative intensity of the intraprotein phonons will be smaller. These arguments suggest that the collective vibrational motions within the protein, especially within the secondary structure, may be closely related to the onset of lysozyme’s enzymatic function, while the interprotein motions are not related to the biological function of lysozyme so closely.

For both of the cases studied here, we find the protein samples with strong enzymatic activity are “soft”; in other words, they have the so-called “conformation flexibility”. Here, we refer this term to the low frequency and large amplitude short-time intraprotein collective vibrational motions, i.e., the small intraprotein phonon energy and large phonon population. In a previous study, Zaccai defined the “softness” and “conformational flexibility” in a mechanical way<sup>61</sup> and tried to relate them to the biological function and activity of the proteins. In this paper, we bring new insight to these two notions in terms of the short-time collective vibrational motion inside protein molecules (especially inside the secondary structures of the proteins). And for the two cases discussed here, such “softness” and “conformational flexibility” are strongly correlated to the onset of the biological function of lysozyme.

## CONCLUSIONS

We investigated the hydration level and temperature effects on the short-time collective vibrational motions in hydrated lysozyme powders with the inelastic X-ray scattering technique. Both hydration level and temperature can be used to switch on and off the enzymatic function of lysozyme without changing its molecular structure significantly. Hence, this experiment allows us to correlate features of the measured IXS spectra with the enzymatic activity of lysozyme. The measured spectra were analyzed using the GTEE theory with satisfactory results. We have identified a well-defined softening of the phonon energies and an enhancement of the phonon population within a particular  $Q$  range when crossing the threshold hydration level  $h = 0.2$ –0.25 from below at  $T = 300$  K. Similar phonon energy softening and population enhancement also exist when crossing the dynamical transition temperature  $T_D$  from below at  $h = 0.33$ . These phenomena indicate that, for the lysozyme samples with native three-dimensional molecular structure, there may exist a correlation between the intraprotein short-time collective vibrational motions and the establishment of the enzymatic function of lysozyme. Collective modes observed in the  $Q$  range of about 15–30  $\text{nm}^{-1}$  seem to be most sensitive to the establishment of enzymatic function of lysozyme. The  $Q$  values in this range correspond to length scales of about 2–4 Å, which are close to the spatial order of the secondary structures of lysozyme. Thus, we conjecture that the motions corresponding to the above-mentioned  $Q$  range are mainly the short-time vibrational collective motions of the secondary structures of lysozyme. Furthermore, since it is found that the samples with



strong enzymatic function exhibit low-frequency and large amplitude intraprotein collective vibrational motions, this “softness” can be taken as a defining characteristic of the “conformational flexibility” that is believed to be essential for the establishment of enzymatic activity in protein.

## AUTHOR INFORMATION

### Corresponding Author

\*E-mail: sowhsin@mit.edu.

### Notes

The authors declare no competing financial interest.

## ACKNOWLEDGMENTS

The research at MIT was supported by a grant from Basic Energy Sciences Division of US DOE DE-FG02-90ER45429. The work at the Advanced Photon Source is supported by the U.S. Department of Energy, Office of Science, Office of Basic Energy Sciences, under Contract No. DE-AC02-06CH11357. E.F. and P.B. acknowledge financial support from Ministero dell'Istruzione, dell'Università e della Ricerca Scientifica (MiUR, grant PRIN-2008, prot. 20087K9A2J, and FIRB-RBPR05JH2P007 Italianonet), and Consorzio Interuniversitario per lo Sviluppo dei Sistemi a Grande Interfase (CSGI).

## REFERENCES

- (1) Crick, F.; Watson, J. Molecular Structure of Nucleic Acids. *Nature* **1953**, *171*, 737–738.
- (2) Linderstrøm-Lang, K.; Schellman, J. In *The Enzymes*; Boyer, P., Lardy, H., Myrback, K., Eds.; Academic Press: New York, 1959.
- (3) Henzler-Wildman, K.; Lei, M.; Thai, V.; Kerns, S.; Karplus, M.; Kern, D. A Hierarchy of Timescales in Protein Dynamics Is Linked to Enzyme Catalysis. *Nature* **2007**, *450*, 913–916.
- (4) Austin, R.; Beeson, K.; Eisenstein, L.; Frauenfelder, H.; Gunsalus, I. Dynamics of Ligand Binding to Myoglobin. *Biochemistry* **1975**, *14*, 5355–5373.
- (5) Ansari, A.; Berendzen, J.; Bowne, S.; Frauenfelder, H.; Iben, I.; Sauke, T.; Shyamsunder, E.; Young, R. Protein States and Proteinquakes. *Proc. Natl. Acad. Sci. U.S.A.* **1985**, *82*, 5000–5004.
- (6) Frauenfelder, H. Conformational Substates in Proteins. *Annu. Rev. Biophys. Chem.* **1988**, *17*, 451–479.
- (7) Frauenfelder, H.; Sligar, S.; Wolynes, P. The Energy Landscapes and Motions of Proteins. *Science* **1991**, *254*, 1598–1603.
- (8) Henzler-Wildman, K.; Kern, D. Dynamic Personalities of Proteins. *Nature* **2007**, *450*, 964–972.
- (9) Frauenfelder, H.; Fenimore, P.; Young, R. Protein Dynamics and Function: Insights from the Energy Landscape and Solvent Slaving. *IUBMB Life* **2007**, *59*, 506–512.
- (10) Ehrenberg, A.; Rigler, R.; Graslund, A.; Nilsson, L., Eds. *Structure, Dynamics and Function of Biomolecules*; Springer-Verlag: 1986; pp 34–38.
- (11) Doster, W.; Cusack, S.; Petry, W. Dynamical Transition of Myoglobin Revealed by Inelastic Neutron Scattering. *Nature* **1989**, *337*, 754–756.
- (12) Doster, W.; Cusack, S.; Petry, W. Dynamic Instability of Liquidlike Motions in a Globular Protein Observed by Inelastic Neutron Scattering. *Phys. Rev. Lett.* **1990**, *65*, 1080–1083.
- (13) Chu, X.; Faraone, A.; Kim, C.; Fratini, E.; Baglioni, P.; Leao, J.; Chen, S. Proteins Remain Soft at Lower Temperatures under Pressure. *J. Phys. Chem. B* **2009**, *113*, 5001–5006.
- (14) Chu, X.; Lagi, M.; Mamontov, E.; Fratini, E.; Baglioni, P.; Chen, S. Experimental Evidence of Logarithmic Relaxation in Single-Particle Dynamics of Hydrated Protein Molecules. *Soft Matter* **2010**, *6*, 2623–2627.
- (15) Roh, J.; Novikov, V.; Gregory, R.; Curtis, J.; Chowdhuri, Z.; Sokolov, A. Onsets of Anharmonicity in Protein Dynamics. *Phys. Rev. Lett.* **2005**, *95*, 38101.
- (16) Mamontov, E.; O'Neill, H.; Zhang, Q. Mean-Squared Atomic Displacements in Hydrated Lysozyme, Native and Denatured. *J. Biol. Phys.* **2010**, *36*, 291–297.
- (17) Wüthrich, K.; Wagner, G. Internal Motion in Globular Proteins. *Trends Biochem. Sci.* **1978**, *3*, 227–230.
- (18) Mittermaier, A.; Kay, L. New Tools Provide New Insights in NMR Studies of Protein Dynamics. *Science* **2006**, *312*, 224.
- (19) Lichtenegger, H.; Doster, W.; Kleinert, T.; Birk, A.; Sepiol, B.; Vogl, G. Heme-Solvent Coupling: a Mössbauer Study of Myoglobin in Sucrose. *Biophys. J.* **1999**, *76*, 414–422.
- (20) Parak, F.; Knapp, E.; Kuchida, D. Protein Dynamics: Mössbauer Spectroscopy on Deoxymyoglobin Crystals. *J. Mol. Biol.* **1982**, *161*, 177–194.
- (21) Schirò, G.; Caronna, C.; Natali, F.; Koza, M.; Cupane, A. The “Protein Dynamical Transition” Does Not Require the Protein Polypeptide Chain. *J. Phys. Chem. Lett.* **2011**, *2*, 2275–2279.
- (22) He, Y.; Ku, P.; Knab, J.; Chen, J.; Markelz, A. Protein Dynamical Transition Does Not Require Protein Structure. *Phys. Rev. Lett.* **2008**, *101*, 178103.
- (23) Ruocco, G.; Sette, F. The High-Frequency Dynamics of Liquid Water. *J. Phys.: Condens. Matter* **1999**, *11*, R259.
- (24) Liu, D.; Chu, X.; Lagi, M.; Zhang, Y.; Fratini, E.; Baglioni, P.; Alatas, A.; Said, A.; Alp, E.; Chen, S. Studies of Phononlike Low-Energy Excitations of Protein Molecules by Inelastic X-Ray Scattering. *Phys. Rev. Lett.* **2008**, *101*, 135501.
- (25) Li, M.; Chu, X.; Fratini, E.; Baglioni, P.; Alatas, A.; Alp, E.; Chen, S. Phonon-Like Excitation in Secondary and Tertiary Structure of Hydrated Protein Powders. *Soft Matter* **2011**, *7*, 9848–9853.
- (26) Yoshida, K.; Hosokawa, S.; Baron, A.; Yamaguchi, T. Collective Dynamics of Hydrated b-Lactoglobulin by Inelastic X-Ray Scattering. *J. Chem. Phys.* **2010**, *133*, 134501.
- (27) Leu, B.; Alatas, A.; Sinn, H.; Alp, E.; Said, A.; Yavas, H.; Zhao, J.; Sage, J.; Sturhahn, W. Protein Elasticity Probed with Two Synchrotron-Based Techniques. *J. Chem. Phys.* **2010**, *132*, 085103.
- (28) Fak, B.; Dorner, B. Institute Laue Langevin (Grenoble, France) Technical Report No 92FA008S; 1992.
- (29) Liao, C.; Chen, S. Theory of the Generalized Dynamic Structure Factor of Polyatomic Molecular Fluids Measured by Inelastic X-Ray Scattering. *Phys. Rev. E* **2001**, *64*, 021205.
- (30) Blake, C.; Koenig, D.; Mair, G.; North, A.; Phillips, D.; Sarma, V. Structure of Hen Egg-White Lysozyme: A Three-dimensional Fourier Synthesis at 2 Å Resolution. *Nature* **1965**, *206*, 757–761.
- (31) Blake, C.; Mair, G.; North, A.; Phillips, D.; Sarma, V. On the Conformation of the Hen Egg-White Lysozyme Molecule. *Proc. R. Soc. London, Ser. B* **1967**, *167*, 365–377.
- (32) Nester, E.; Anderson, D.; Roberts, J. C. E. *Microbiology: A Human Perspective*, 7th ed.; McGraw-Hill Science/Engineering/Math: 2011.
- (33) Sinn, H.; Alp, E.; Alatas, A.; Barraza, J.; Bortel, G.; Burkel, E.; Shu, D.; Sturhahn, W.; Sutter, J.; Toellner, T. An Inelastic X-Ray Spectrometer With 2.2 meV Energy Resolution. *Nucl. Instrum. Methods Phys. Res., Sect. A* **2001**, *467*, 1545–1548.
- (34) Alatas, A.; Leu, B.; Zhao, J.; Yavas, H.; Toellner, T.; Alp, E. Improved Focusing Capability for Inelastic X-ray Spectrometer at 3-ID of the APS: A Combination of Toroidal and Kirkpatrick-Baez (KB) Mirrors. *Nucl. Instrum. Methods Phys. Res., Sect. A* **2011**, *649*, 166–168.
- (35) Toellner, T.; Alatas, A.; Said, A. Six-Reflection meV-Monochromator for Synchrotron Radiation. *J. Synchrotron Radiat.* **2011**, *18*, 605–611.
- (36) De Schepper, I.; Cohen, E.; Bruin, C.; van Rijs, J.; Montfrooij, W.; de Graaf, L. Hydrodynamic Time Correlation Functions for a Lennard-Jones Fluid. *Phys. Rev. A* **1988**, *38*, 271.
- (37) Chen, S.; Liao, C.; Huang, H.; Weiss, T.; Bellisent-Funel, M.; Sette, F. Collective Dynamics in Fully Hydrated Phospholipid Bilayers Studied by Inelastic X-Ray Scattering. *Phys. Rev. Lett.* **2001**, *86*, 740–743.
- (38) Chen, P.; Liu, Y.; Weiss, T.; Huang, H.; Sinn, H.; Alp, E.; Alatas, A.; Said, A.; Chen, S. Studies of Short-Wavelength Collective

Molecular Motions in Lipid Bilayers Using High Resolution Inelastic X-ray Scattering. *Biophys. Chem.* **2003**, *105*, 721–741.

(39) Liu, Y.; Berti, D.; Faraone, A.; Chen, W.; Alatas, A.; Sinn, H.; Alp, E.; Said, A.; Baglioni, P.; Chen, S. Inelastic X-Ray Scattering Studies of Phonons in Liquid Crystalline DNA. *Phys. Chem. Chem. Phys.* **2004**, *6*, 1499–1505.

(40) Liu, Y.; Berti, D.; Baglioni, P.; Chen, S.; Alatas, A.; Sinn, H.; Said, A.; Alp, E. Inelastic X-Ray Scattering Studies of Phonons Propagating Along the Axial Direction of a DNA Molecule Having Different Counter-Ion Atmosphere. *J. Phys. Chem. Solids* **2005**, *66*, 2235–2245.

(41) Liu, Y.; Chen, S.; Berti, D.; Baglioni, P.; Alatas, A.; Sinn, H.; Alp, E.; Said, A. Effects of Counterion Valency on the Damping of Phonons Propagating Along the Axial Direction of Liquid-Crystalline DNA. *J. Chem. Phys.* **2005**, *123*, 214909.

(42) Squires, G. L. *Introduction to the Theory of Thermal Neutron Scattering*; Dover: New York, 1996.

(43) Hansen, J.; McDonald, I. *Theory of Simple Liquids*; Academic Press: 2006.

(44) De Gennes, P. Liquid Dynamics and Inelastic Scattering of Neutrons. *Physica* **1959**, *25*, 825–839.

(45) Chen, S.; Kotlarchyk, M. *Interactions of Photons and Neutrons with Matter*, 2nd ed.; World Scientific: 2007.

(46) Etchegoin, P. Glassylike Low-Frequency Dynamics of Globular Proteins. *Phys. Rev. E* **1998**, *58*, 845.

(47) Careri, G.; Gratton, E.; Yang, P.; Rupley, J. Correlation of IR Spectroscopic, Heat Capacity, Diamagnetic Susceptibility and Enzymatic Measurements on Lysozyme Powder. *Nature* **1980**, *284*, 572–573.

(48) Rupley, J.; Gratton, E.; Careri, G. Water and Globular Proteins. *Trends Biochem. Sci.* **1983**, *8*, 18–22.

(49) Orecchini, A.; Paciaroni, A.; Francesco, A.; Petrillo, C.; Sacchetti, F. Collective Dynamics of Protein Hydration Water by Brillouin Neutron Spectroscopy. *J. Am. Chem. Soc.* **2009**, *131*, 4664–4669.

(50) Paciaroni, A.; Orecchini, A.; Haertlein, M.; Moulin, M.; Conti Nibali, V.; De Francesco, A.; Petrillo, C.; Sacchetti, F. Vibrational Collective Dynamics of Dry Proteins in the Terahertz Region. *J. Phys. Chem. B* **2012**, *116*, 3861–3865.

(51) Wang, H.; Ben-Naim, A. Solvation and Solubility of Globular Proteins. *J. Phys. Chem. B* **1997**, *101*, 1077–1086.

(52) Doster, W.; Settles, M. Protein–Water Displacement Distributions. *Biochim. Biophys. Acta, Proteins Proteomics* **2005**, *1749*, 173–186.

(53) Lagi, M.; Baglioni, P.; Chen, S. Logarithmic Decay in Single-Particle Relaxation of Hydrated Lysozyme Powder. *Phys. Rev. Lett.* **2009**, *103*, 108102.

(54) Tarek, M.; Tobias, D. Single-Particle and Collective Dynamics of Protein Hydration Water: A Molecular Dynamics Study. *Phys. Rev. Lett.* **2002**, *89*, 275501.

(55) Batzer, H.; Kreibich, U. Influence of Water on Thermal Transitions in Natural Polymers and Synthetic Polyamides. *Polym. Bull.* **1981**, *5*, 585–590.

(56) Rasmussen, B.; Stock, A.; Ringe, D.; Petsko, G. Crystalline Ribonuclease A Loses Function Below the Dynamical Transition at 220 K. *Nature* **1992**, *357*, 423–424.

(57) Higgins, J.; Benoit, H. *Polymers and Neutron Scattering*; Oxford University Press: 1997.

(58) [http://en.wikipedia.org/wiki/Protein\\_secondary\\_structure](http://en.wikipedia.org/wiki/Protein_secondary_structure).

(59) Brooks, B.; Karplus, M. Normal Modes for Specific Motions of Macromolecules: Application to the Hinge-Bending Mode of Lysozyme. *Proc. Natl. Acad. Sci. U.S.A.* **1985**, *82*, 4995–4999.

(60) He, Y.; Chen, J.; Knab, J.; Zheng, W.; Markelz, A. Evidence of Protein Collective Motions on the Picosecond Timescale. *Biophys. J.* **2011**, *100*, 1058–1065.

(61) Zaccai, G. How Soft Is a Protein? A Protein Dynamics Force Constant Measured by Neutron Scattering. *Science* **2000**, *288*, 1604–1607.